Preprints.org

Article

Not peer-reviewed version

Optical Angular Momentum Beam Generation Using Coherent Beam Combination

Przemyslaw Gontar , Jan Jabczyński * , Lukasz Gorajek , Waldemar Zendzian

Posted Date: 22 August 2024

doi: 10.20944/preprints202408.1484.v1

Keywords: laser beams; coherent beam combining; optical angular momentum; vortex beams; free space optical communications

Preprints.org is a free multidiscipline platform providing preprint service that is dedicated to making early versions of research outputs permanently available and citable. Preprints posted at Preprints.org appear in Web of Science, Crossref, Google Scholar, Scilit, Europe PMC.

Copyright: This is an open access article distributed under the Creative Commons Attribution License which permits unrestricted use, distribution, and reproduction in any medium, provided the original work is properly cited.

Preprints.org (www.preprints.org) | NOT PEER-REVIEWED | Posted: 22 August 2024 doi:10.20944/preprints202408.1484.v1

Disclaimer/Publisher's Note: The statements, opinions, and data contained in all publications are solely those of the individual author(s) and contributor(s) and not of MDPI and/or the editor(s). MDPI and/or the editor(s) disclaim responsibility for any injury to people or property resulting from any ideas, methods, instructions, or products referred to in the content.

Article

Optical Angular Momentum Beam Generation Using Coherent Beam Combination

Przemyslaw Gontar, Lukasz Gorajek, Waldemar Zendzian and Jan Jabczyński *

Military University of Technology, Institute of Optoelectronics, ul. gen. S. Kaliskiego 2, 00-908 Warsaw, Poland

* Correspondence: jan.jabczynski@wat.edu.pl; Tel.: +48 -261-839-617 (J.J.)

Abstract: (1) Background: The significant progress observed over last two decades in coherent beam combining (CBC) technology has mainly focused on its applications in high-energy physics and laser weapons. This work provides insight into the basic principles of CBC and the search for an alternative, namely optical angular momentum (OAM) generation using CBC; (2) Methods: The semi-analytical model based on the paraxial wave equation explored generating OAM-CBC beams by manipulating the tilts and phases of CBC (T&P-CBC) of hexagonal architecture; (3) Results: The specially arranged T&P-CBC shows typical properties of OAM, such as annular profiles for the zero diffraction order and 1-st order replicas in the far field and correlation coefficients of 1% between different OAM-CBC fields; (4) Conclusions: The differences between classical OAM beams and OAM-CBC are substantial due to hexagonal lattice properties. Moreover, applications in free space optical communications are feasible as T&P CBC fulfills the main conditions and requirements for OAM generation.

Keywords: laser beams; coherent beam combining; optical angular momentum; vortex beams; free space optical communications

1. Introduction

Coherent beam combination (CBC) technology, including filled aperture CBC (FA-CBC) and tiled aperture CBC (TA-CBC) [1–11], has been developed in the last two decades, mainly for applications in laser weapons [4,12] and high energy physics [6,10]. FA-CBC offers high efficiency and robustness but it is limited by the number of emitters (not higher than 12 beams was demonstrated for high average power system [13]). In contrast, TA-CBC offers direct scalability beyond hundreds of combined beams, but has low practical efficiency [5,10,11], and difficulty scaling to high average powers. Both technologies require effective adaptive optics subsystems for outdoor applications, such as laser weapons and free-space optical communications (FSOC), over long propagation distances in horizontal directions [8,9,14,15] and/or in Earth-satellite FSOC links [16–18].

Since the 1990s, optical angular momentum (OAM) beams have been examined theoretically and experimentally, attracting [19–23] growing interest in material processing, optical tweezing and FSOC [16,18,23–27]. The benefits of OAM technology include propagation invariance as 'diffraction-free' solutions of paraxial wave equation, enhanced resilience to atmospheric turbulence, and orthogonality, enabling potential increase in FSOC channel bandwidth thanks to spatial multiplexling. However, its scalability in power and practical realization in laboratory and outdoor applications are problematic for a single aperture output.

The purpose of this study was to merge both technologies, that is, to search for the possibilities of CBC technology for generation of OAM beams (OAM-CBC). Preliminary results were presented in [28], where a segmented vortex wavefront was constructed in the near field owing to a special helix-like stepped phase shift in the hexagonal lattice. Here, we develop this approach for special type of tilted and phased CBC (T&P-CBC) concept, enabling the effective construction of segmented vortex wavefronts in the near field. Section 2 describes the semi-analytical model of CBC propagation

© 2024 by the author(s). Distributed under a Creative Commons CC BY license.

Preprints.org (www.preprints.org) | NOT PEER-REVIEWED | Posted: 22 August 2024 doi:10.20944/preprints202408.1484.v1

and the
OAM-CBC concept. The main results, analysis, and discussion are presented in Section 3, and conclusions are drawn in Section 4.

2. Tilted and Phased CBC for Optical Angular Momentum generation

Here, we give only a brief description of the analysis method. The full mathematical model is described in detail in [30,31]. To start, we provide the main characteristics of CBC hexagonal architecture (see Figure 1). The center and chief ray directions of each (l, n)-th emitter/beam of the CBC are defined by the geometry of hexagonal lattice; N_{cr} is the number of crowns; $N_{lat} = 3N_{cr}(N_{cr}+1)+1$ is the number of emitters; a is the half period of the lattice; r_a is the sub aperture radius; $f.f. = r_a/a$ is the filling factor, f is the focal length. In the classical CBC configuration, each chief ray is directed to the common focal point F, with a spherical segmented wavefront of CBC lattice of radius f. Diffraction profiles of CBC in the far field are characterized by the Airy radius $r_{Airy} = 0.61\lambda/NA_{lat}$ and Fresnel range $Z_{Fresnel} = \lambda/NA_{lat}^2$, where $NA_{lat} = (N_{cr}+1/2)2a/f$ is the numerical aperture of lattice and λ is the wavelength.

We apply a truncated Gaussian beam as a 'prototype' optical field. To simplify calculations, we used the once determined and calculated approximate solution of a truncated Gaussian beam, for given beam radius w_1 at the aperture and truncation level
$\varepsilon_{tr} = \exp(-2(r_a/w_1)^2)$ (see [32] for details), which is valid over a wide range of propagation distances in the vicinity of focal point F. Note that the ratio of Rayleigh range of an individual beam to the caustics length defined by Fresnel range is proportional to N_{cr}^2. Typically, for long-distance propagation, the Rayleigh range is comparable to f ('collimation case'), whereas the Fresnel range is N_{lat} times shorter. We calculated the coherent sum of all input beams for specific distribution of phases and tilts for a chosen plane near focal point F.

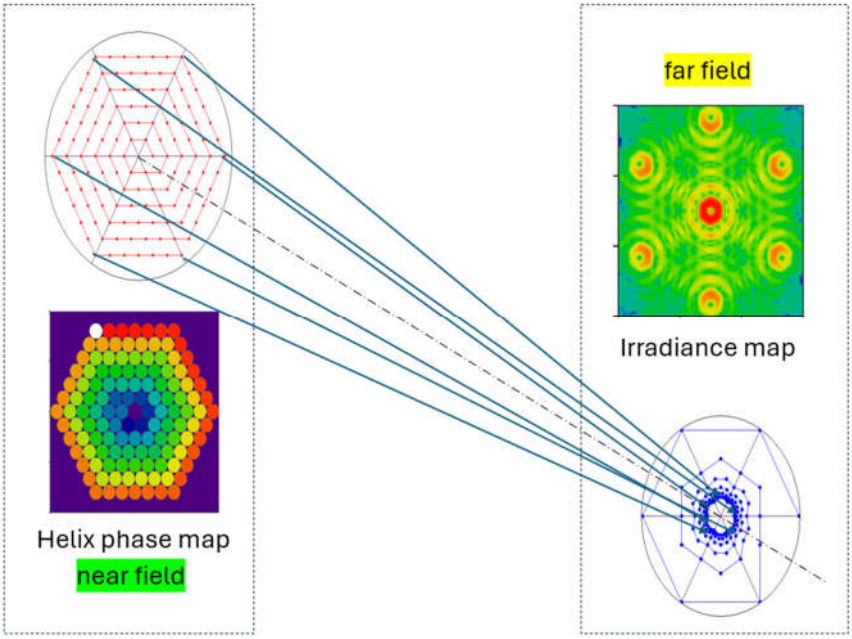

Figure 1. Concept of optical angular momentum-coherent beam combining (OAM-CBC) generation via tilted &phased CBC.

Evidently, various T&P-CBC realizations exist in the $(1+3)\times N_{lat}$ dimensional space of control parameters. Exploration of this subject is far beyond the scope of this study. Here, we focus on the OAM-CBC case. We define a specific segmented vortex wavefront with a step-like helix phase and tilt vector $[\theta_x, \theta_y]$ in the near field as follows:

The OAM-CBC amplitude $B_{m_{\mathrm{OAM}}}$ with given m_{OAM} - optical angular momentum number can be described as follows:

Preprints.org (www.preprints.org) | NOT PEER-REVIEWED | Posted: 22 August 2024 doi:10.20944/preprints202408.1484.v1

$$B_{m_{\mathrm{OAM}}} = \sum_{l,n} A_{l,n} \exp\left[ik\Phi_{l,n}\right] \quad \text{where} \quad \Phi_{l,n} = \frac{r_{l,n}^{\,2}}{f} + m_{\mathrm{OAM}} \frac{\varphi_{l,n}}{k} \qquad (1)$$

Here, l and n are the indices of the sub-aperture, $A_{l,n}$ is the amplitude of (l,n) sub-aperture, $r_{l,n}$ and $\varphi_{l,n}$ are the radius to the lattice center and azimuth angle of each sub-aperture, f is the focal length, k is the wavenumber.

Next, we calculate vortex tilt vector $[\theta_x, \theta_y]$ by gradient $\nabla\Phi_{l,n}$ as follows:

$$\nabla\Phi_{l,n} = \left[\theta_{x,l,n}, \theta_{y,l,n}\right] = \left[\frac{r_{l,n}\cos\varphi_{l,n}}{f} + m_{\mathrm{OAM}}\frac{\sin\varphi_{l,n}}{kr_{l,n}} \quad , \quad \frac{r_{l,n}\sin\varphi_{l,n}}{f} - m_{\mathrm{OAM}}\frac{\cos\varphi_{l,n}}{kr_{l,n}}\right] \qquad (2)$$

Note, that for $m_{\mathrm{OAM}} \neq 0$ the geometrical-optics caustics of OAM-CBC vortex segmented wavefront has a coiling non-linear helix shape with an inner hole (lower right part of Figure 1) corresponding to the evolving hexagonal helix of the CBC in the near field (upper left part in Figure 1). The coiling helix for $m_{\mathrm{OAM}}=0$ transforms into a distinct focal point F for classical spherical CBC case. This phenomenon is a direct geometrical-optics interpretation of vanishing irradiance at $r = 0$ and annular amplitude distribution in caustics for vortex OAM beam.

3. Results

We tested the proposed OAM-CBC concept for a large hexagonal lattice consisted of N_{cr}= 6 outer crowns (N_{lat}=127 emitters), assuming very dense packing ($f.f.$=0.99). To neglect the peculiarities of diffraction, we assumed low truncation losses ε_{tr}=0.05. Thus, an "almost" Gaussian beam is emitted by an individual emitter with a very low power content at higher diffraction orders in the caustics region. The hexagonal architecture of the CBC reflects the six-folded symmetry of 1-st diffraction orders (see Figure 2).

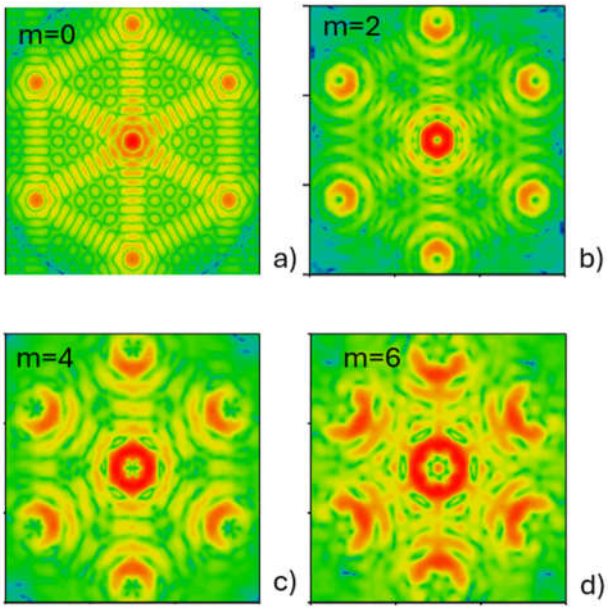

Figure 2. 2D maps of OAM-CBC irradiance distributions (in logarithmic scale) in the far field for optical angular momentum number; a) m_{OAM} =0; b) 2; c) 4; d) 6; N_{lat}=127, $f.f.$ =0.99, ε_{tr}=0.05.

The basic compliance between the geometrical-optics caustics (Figure 1) and wave-optics demonstrate a dominant annular profile in the zero-order diffraction area (Figure 2,3, and 4). In Figure 2 the irradiance maps for $m_{\mathrm{OAM}} > 0$ (Figure 2b-d) exhibit the expected properties of the conjunction of CBC and OAM beams. The zero-diffraction order has a nearly annular shape and 1-st diffraction orders resemble its replicas.

The typical dependencies of the far field profiles and power in bucket (PIB) curves for OAM-CBC are shown in Figure 3 and 4.

Preprints.org (www.preprints.org) | NOT PEER-REVIEWED | Posted: 22 August 2024 doi:10.20944/preprints202408.1484.v1

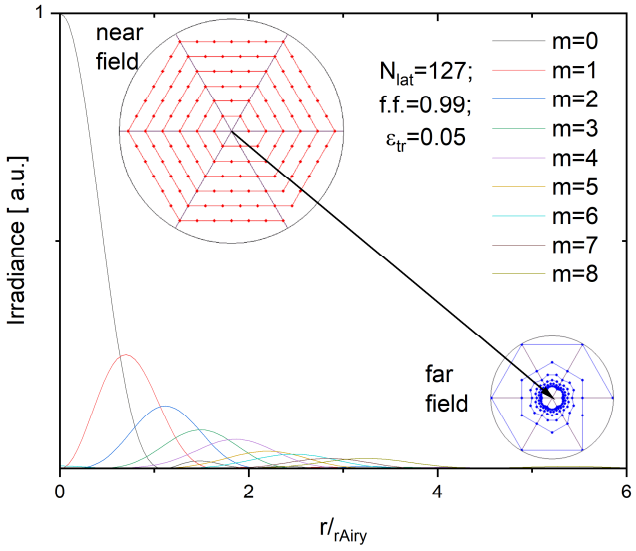

Figure 3. Irradiance profiles in the far field for m_{OAM} ϵ (0,8); *f.f.*=0.99 , ε_{tr}=0.05, N_{lat}=127.

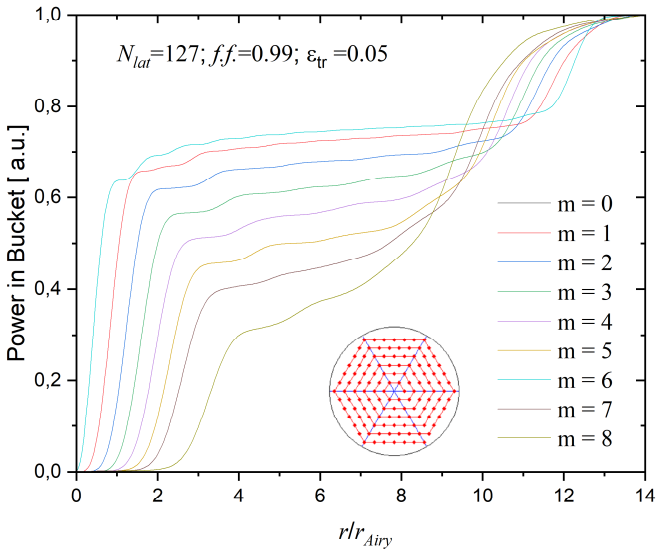

Figure 4. Power in buckets curves for m_{OAM} ϵ (0,8); *f.f.*=0.99, ε_{tr}=0.05, N_{lat}=127.

With an increase in m_{OAM}, the amplitude profiles worsen with flattening and dissipation of power density out of the low diffraction lobes (Figs. 3, 4). Moreover, above m_{OAM} >5, the 2D maps resemble the aberrated and scattered partly coherent beams with the minimum at the axis. These features are particularly highlighted for m_{OAM} =6 (Figure 2d), for which six-fold symmetries of the vortex and hexagonal lattice overlap.

To examine the orthogonality of a set of OAM-CBC amplitude profiles in the far field and the feasibility in FSOC, we have calculated correlation coefficients $\gamma_{m,k}$ defined as follows:

$$\gamma_{m,k} = \frac{\langle B_m B_k^* \rangle}{\sqrt{\langle B_m B_m^* \rangle \langle B_k B_k^* \rangle}} \qquad (3)$$

where $\langle B_m B_k^* \rangle$ denotes the discrete 2D summation of $B_m B_k^*$ over finite area in the far field; (15 x 15 r_{Airy} in our case).

Preprints.org (www.preprints.org) | NOT PEER-REVIEWED | Posted: 22 August 2024 doi:10.20944/preprints202408.1484.v1

The results of $\gamma_{m,k}$ calculations for a trail of 9 configurations with $m_{\mathrm{OAM}} \in (0,8)$ are collected in Table 1.

Table 1. Correlation coefficients for OAM-CBC amplitude profiles in the far field; $m_{\mathrm{OAM}} \in (0,8)$, *f.f.*=0.99, ε_{tr}=0.05, N_{lat}=127.

m_{OAM}	0	1	2	3	4	5	6	7	8
0	1.00000	0.00844	0.00875	0.00924	0.00986	0.01000	**0.10100**	0.01200	0.01200
1	0.00844	1.00000	**0.00484**	0.00507	0.00541	0.00570	0.00848	0.08800	0.00701
2	0.00875	0.00484	1.00000	0.00530	0.00562	0.00599	0.00862	0.00681	0.09500
3	0.00924	0.00507	0.00530	1.00000	0.00592	0.00621	0.00918	0.00770	0.00768
4	0.00986	0.00541	0.00562	0.00592	1.00000	0.00669	0.00958	0.00761	0.00843
5	0.01000	0.00570	0.00599	0.00621	0.00669	1.00000	0.01000	0.00846	0.00868
6	0.10100	0.00848	0.00862	0.00918	0.00958	0.01000	1.00000	0.01100	0.01200
7	0.01200	0.08800	0.00681	0.00770	0.00761	0.00846	0.01100	1.00000	0.00987
8	0.01200	0.00701	0.09500	0.00768	0.00843	0.00868	0.01200	0.00987	1.00000

Nonperfect orthogonality is caused by the characteristics of OAM-CBC concept (discrete 2D array of hexagonal symmetry), numerical errors, approximate solution of truncated Gaussian beam, and discrete summation over limited area.

The values of $\gamma_{m,k}$ were in range [0.0048, 0.1]. For a narrow range of $m_{\mathrm{OAM}} \in (0,5)$ average correlation coefficient $\gamma_{m,k}$ = 0.7%, whereas for a $m_{\mathrm{OAM}} \in (0,8)$ it increases to 1.5%. We suppose that a correlation coefficient of 1%, corresponding to the cross-channel crosstalk, is acceptable for practical applications in FSOC. Thus, we can conclude that the T&P-CBC sufficiently satisfies the main conditions and requiremnets of OAM generation.

4. Conclusions

Numerical experiments demonstrated the feasibility of merging of OAM and CBC technologies. For a densely packed CBC hexagonal array, the vortex wavefront was emulated with a step-like evolving helix of phase and tilts vectors in the near field.

i/ The irradiance maps for $m_{\mathrm{OAM}} > 0$ exhibit the expected properties of combination of CBC and OAM beams. The zero-diffraction order has a nearly annular shape and 1-st diffraction orders resemble its replicas. However, the differences between classical OAM beams and OAM-CBC are substantial owing to their hexagonal lattice properties.

ii/ The imperfect orthogonality of OAM-CBC set is attributed to the specfic characteristics of OAM-CBC concept (discrete 2D array of hexagonal symmetry), numerical errors, and discrete

Preprints.org (www.preprints.org) | NOT PEER-REVIEWED | Posted: 22 August 2024 doi:10.20944/preprints202408.1484.v1

summation over a limited area. For the m_{OAM} range of (0,5) the average correlation coefficient, corresponding to cross-channel crosstalk, is 0.7%, which is acceptable for practical applications in FSOC.

We conclude that the proposed here T&P-CBC concept fulfills the primary conditions and requirements for OAM generation. In further research we intend to examine the rules of OAM-CBC algebra and the impact of lattice architecture parameters and imprefections.

Supplementary Materials: no supplement

Author Contributions: Conceptualization, J.J. and W.Z.; methodology, L.G, W.Z. and J.J; software, P.G. and G.L.; data curation, P.G. ; writing—J.J.; writing—review and editing, P.G.. and J.J.; visualization, G.P..; supervision, J.J.

Funding: This research received no external funding.

Data Availability Statement: Dataset available on request from the authors

Acknowledgments: We would like to express our gratitude to Dr Janusz Mikołajczyk and Mr. Aluś Emo Capodilista for helpful support and discussion.

Conflicts of Interest: The authors declare no conflicts of interest.

References

1. Brignon, A. *Coherent Laser Beam Combining*, Ed.; 2013th ed.; Wiley-VCH, Verlag GmbH & Co. KGaA , **2013**; ISBN 978-3-527-65280-8.
2. Fathi, H.; Närhi, M.; Gumenyuk, R. Towards Ultimate High-Power Scaling: Coherent Beam Combining of Fiber Lasers. *Photonics* **2021**, *8*, 566, doi:10.3390/photonics8120566
3. Fan, T.Y. Laser Beam Combining for High-Power, High-Radiance Sources. *IEEE Journal on Selected Topics in Quantum Electronics* **2005**, *11*, 567–577, doi:10.1109/JSTQE.2005.850241.
4. Van Zandt, N.R.; Cusumano, S.J.; Bartell, R.J.; Basu, S.; McCrae, J.E.; Fiorino, S.T. Comparison of Coherent and Incoherent Laser Beam Combination for Tactical Engagements. *Optical Engineering* **2012**, *51*, 104301, doi:10.1117/1.oe.51.10.104301.
5. Shpakovych, M.; Maulion, G.; Kermene, V.; Boju, A.; Armand, P.; Desfarges-Berthelemot, A.; Barthélemy, A. Experimental Phase Control of a 100 Laser Beam Array with Quasi-Reinforcement Learning of a Neural Network in an Error Reduction Loop. *Opt Express* **2021**, *29*, 12307, doi:10.1364/oe.419232.
6. Mourou, G.; Brocklesby, B.; Tajima, T.; Limpert, J. The Future Is Fibre Accelerators. *Nat Photonics* **2013**, *7*, 258–261.
7. Leshchenko, V.E. Coherent Combining Efficiency in Tiled and Filled Aperture Approaches. *Opt Express* **2015**, *23*, 15944, doi:10.1364/oe.23.015944.
8. Jabczyński, J.K.; Gontar, P. Impact of Atmospheric Turbulence on Coherent Beam Combining for Laser Weapon Systems. *Defence Technology* **2021**, *17*, 1160–1167, doi:10.1016/j.dt.2020.06.021.
9. Weyrauch, T.; Vorontsov, M.; Mangano, J.; Ovchinnikov, V.; Bricker, D.; Polnau, E.; Rostov, A. Deep Turbulence Effects Mitigation with Coherent Combining of 21 Laser Beams over 7 Km. *Opt Lett* **2016**, *41*, 840, doi:10.1364/ol.41.000840.
10. Fsaifes, I.; Daniault, L.; Bellanger, S.; Veinhard, M.; Bourderionnet, J.; Larat, C.; Lallier, E.; Durand, E.; Brignon, A.; Chanteloup, J.-C. Coherent Beam Combining of 61 Femtosecond Fiber Amplifiers. *Opt Express* **2020**, *28*, 20152, doi:10.1364/OE.394031.
11. Chang, H.; Chang, Q.; Xi, J.; Hou, T.; Su, R.; Ma, P.; Wu, J.; Li, C.; Jiang, M.; Ma, Y.; et al. First Experimental Demonstration of Coherent Beam Combining of More than 100 Beams. *Photonics Res* **2020**, *8*, 1943, doi:10.1364/prj.409788.
12. Sprangle, P.; Ting, A.; Peñano, J.; Fischer, R.; Hafizi, B. Incoherent Combining and Atmospheric Propagation of High-Power Fiber Lasers for Directed-Energy Applications. *IEEE J Quantum Electron* **2009**, *45*, 138–148, doi:10.1109/JQE.2008.2002501.
13. Müller, M.; Aleshire, C.; Klenke, A.; Haddad, E.; Légaré, F.; Tünnermann, A.; Limpert, J. 10.4 KW Coherently Combined Ultrafast Fiber Laser. *Opt Lett* **2020**, *45*, 3083, doi:10.1364/ol.392843.
14. Vorontsov, M.; Filimonov, G.; Ovchinnikov, V.; Polnau, E.; Lachinova, S.; Weyrauch, T.; Mangano, J. Comparative Efficiency Analysis of Fiber-Array and Conventional Beam Director Systems in Volume Turbulence. *Appl Opt* **2016**, *55*, 4170, doi:10.1364/ao.55.004170.
15. Weyrauch, T.; Vorontsov, M.A.; Carhart, G.W.; Beresnev, L.A.; Rostov, A.P.; Polnau, E.E.; Liu, J.J. Experimental Demonstration of Coherent Beam Combining over a 7 Km Propagation Path. *Opt Lett* **2011**, *36*, 4455-4457.

Preprints.org (www.preprints.org) | NOT PEER-REVIEWED | Posted: 22 August 2024 doi:10.20944/preprints202408.1484.v1

16. Meric, H. *Atmospheric Turbulence Modeling and Aperture Analysis for Optimizing Receiver Design and System Performance on Free Space Optical Communication Links*; PhD Thesis, **2012**.
17. Andrews, L.C.; Phillips, R.L. *Laser Beam Propagation through Random Media*; SPIE, **2005**; ISBN 0-8194-5948-8.
18. Stotts, L.B.; Andrews, L.C. Optical Communications in Turbulence: A Tutorial. *Optical Engineering* **2023**, *63*, doi:10.1117/1.oe.63.4.041207.
19. Allen, L.; Barnett, S.M.; Padgett, M.J. *Optical Angular Momentum*; CRC Press, **2016**; ISBN 9781482269017.
20. Lian, Y.; Qi, X.; Wang, Y.; Bai, Z.; Wang, Y.; Lu, Z. OAM Beam Generation in Space and Its Applications: A Review. *Opt Lasers Eng* **2022**, *151*.
21. Shiri, A.; Gbur, G. Orbital Angular Momentum Spectrum of Model Partially Coherent Beams in Turbulence. *Opt Express* **2024**, *32*, 18175, doi:10.1364/oe.523635.
22. Hou, T.; Zhang, Y.; Chang, Q.; Ma, P.; Su, R.; Wu, J.; Ma, Y.; Zhou, P. High-Power Vortex Beam Generation Enabled by a Phased Beam Array Fed at the Nonfocal-Plane. *Opt Express* **2019**, *27*, 4046, doi:10.1364/oe.27.004046.
23. Yu, T.; Xia, H.; Xie, W.; Peng, Y. Orbital Angular Momentum Mode Detection of the Combined Vortex Beam Generated by Coherent Combining Technology. *Opt Express* **2020**, *28*, 35795, doi:10.1364/oe.409122.
24. Vetter, C.; Steinkopf, R.; Bergner, K.; Ornigotti, M.; Nolte, S.; Gross, H.; Szameit, A. Realization of Free-Space Long-Distance Self-Healing Bessel Beams. *Laser Photon Rev* **2019**, *13*, doi:10.1002/lpor.201900103.
25. Rouzé, B.; Lombard, L.; Jacqmin, H.; Liméry, A.; Durécu, A.; Bourdon, P. Coherent Beam Combination of Seven 1.5 Mm Fiber Amplifiers through up to 1 Km Atmospheric Turbulence: Near- and Far-Field Experimental Analysis. *Appl Opt* **2021**, *60*, 8524, doi:10.1364/ao.433872.
26. Doster, T.; Watnik, A.T. Laguerre–Gauss and Bessel–Gauss Beams Propagation through Turbulence: Analysis of Channel Efficiency. *Appl Opt* **2016**, *55*, 10239, doi:10.1364/ao.55.010239.
27. Fiorino, S.T.; Bartell, R.J.; Krizo, M.J.; Caylor, G.L.; Moore, K.P.; Harris, T.R.; Cusumano, S.J. A First Principles Atmospheric Propagation & Characterization Tool: The Laser Environmental Effects Definition and Reference (LEEDR). In Proceedings of the Atmospheric Propagation of Electromagnetic Waves II; SPIE, February 7 2008; Vol. 6878, p. 68780B.
28. Jabczynski, J.K.; Gontar, P.; Gorajek, L.; Zendzian, W. Segmented Vortex Wavefront Coherent Beam Combining. *AIP Adv* **2022**, *12*, doi:10.1063/5.0084945.
29. Jabczyński, J.K. Bessel-Gauss Coherently Combined Beams. *Opt Express* **2024**, *32*, 10068, doi:10.1364/oe.518686.
30. Jabczynski, J.K.; Gontar, P. Analysis of the Caustics of Partially Coherently Combined Truncated Gaussian Beams. *Appl Opt* **2020**, *59*, 3340, doi:10.1364/ao.389415.
31. Jabczyński, J.K.; Gontar, P.; Gorajek, Ł.; Żendzian, W. Simplified Sensitivity Analysis of Coherent Beam Combining in a Tiled Aperture Architecture. *Appl Opt* **2021**, *60*, 5012–5019, doi:10.1364/ao.421856.
32. Ding, D.; Liu, X. Approximate Description for Bessel, Bessel-Gauss, and Gaussian Beams with Finite Aperture. *J. Opt Soc Am A* **1999**, *16*, 1286–1293; doi:10.1364/JOSAA.16.001286.

Disclaimer/Publisher's Note: The statements, opinions and data contained in all publications are solely those of the individual author(s) and contributor(s) and not of MDPI and/or the editor(s). MDPI and/or the editor(s) disclaim responsibility for any injury to people or property resulting from any ideas, methods, instructions or products referred to in the content.